

Finite element analysis of the dynamic behavior of concrete-filled double skin steel tubes (CFDST) under lateral impact with fixed-simply support

M. Liu & R. Wang

*Architecture and Civil Engineering,
Taiyuan University of Technology, China*

Abstract

Concrete-filled double skin steel tubes (CFDST) are a type of steel-concrete composite structure. This structure has been widely used in high-rise buildings, bridges and power facilities. The current research about it focuses on the performance about axial compression, bias, bending, and low cyclic loads. However, during the whole life cycle, these structures may inevitably suffer from various impact loads. In order to understand the dynamic response of these structures under lateral impact, this paper sets up a finite element model to analyze the destruction modal, impact force (F), deflection (Δ) as well as other dynamic responses of CFDST under lateral impact load. One end of the CFDST is fixed while the other end is simply supported. The whole process and failure mechanics of the dynamic response of CFDST under lateral impact are analyzed basically, laid the foundation for further parametric analysis and practical calculation method.

Keywords: concrete-filled double skin steel tubes (CFDST), lateral impact load, dynamic response, finite element model analysis.

1 Introduction

Compared with the traditional concrete-filled steel tubes (CFST), concrete-filled double skin steel tubes (CFDST) [1] add a smaller concentric steel tube, and fill the space with concrete between the outer steel tube and the inner steel tube. Since the better bending rigidity, expanding cross-section, seismic and fire



resistance, light weight, CFDST primarily applies as load-bearing components to subway, gymnasium, support columns of offshore platform, piers and other buildings requiring high bearing capability. During the life cycle, these components may inevitably suffer accidental impact. For instance, explosion of meteorite, collision of crashed plane, impact of cars or ships [2]. For example, 50% of bridges in Beijing suffered from vehicle collision. The survey data from Department of Transportation in New York show that there were 520 of 1000 collapsed bridges due to impact, while only 19 of 1000 due to earthquake. Once an accident occurs, the structure may be severely damaged or even completely lose bearing capacity, leading to huge losses of life and property. Therefore, it's necessary to study the dynamic behavior of CFDST under lateral impact load.

Serious literature has been done about CFST's impact performance, e.g. Chen *et al.* [5], Xiao *et al.* [6], Huo *et al.* [7], Bambach [8], Wang *et al.* [9] and Hou [10]. Currently, research about CFDST mainly focus on the static performance of axial compression, pure bending and the hysteretic behavior of bending components, as well as torsional properties of torsion members [11–14]. The experimental analysis and theoretical research of CFDST under lateral impact loading is still relatively less. In this paper, the finite element analysis model of CFDST under lateral impact with fixed-simply support is established by the ABAQUS finite element software. The work mechanic and full range of the dynamic response are analyzed. To verify the correctness of the model, the finite element analysis model of CFST under lateral impact is established firstly, the analysis results are compared with existing experimental results. Then the finite element analysis model of CFDST under lateral impact is built, and the whole process and failure mechanics are analyzed. The results showed that there is a stable platform of impact force of the CFDST under lateral impact with fixed-simply supported and the specimen has a good anti-impact performance.

2 Finite element analysis (FEA) model

Reference to the literature [9], this paper set up the model of CFDST under lateral impact with fixed-simply supported in ABAQUS/Explicit module (Hibbitt, Karlsson & Sorensen Inc.) [17].

2.1 Materials

A five-phase elastic-plastic constitutive model introduced by Han [15] is used herein to simulate the steel, take account of the impact of strength due to the strain rate under dynamic loading, Cowper-Symonds model is employed:

$$\sigma_d / \sigma_s = 1 + (\dot{\epsilon} / D)^{1/p} \quad (1)$$

where, $\dot{\epsilon}$ is strain rate of steel, σ_d is stress value when strain rate of steel is $\dot{\epsilon}$, σ_s is stress of steel under the static stress, D and p are material parameters. In this paper $D=6844s^{-1}$ and $p=3.91$ [10]. For steel, elastic modulus, yield strength and Poisson's ratio is 2.06×10^5 MPa, 298 MPa, 0.3 [9]. For supports, elastic modulus

and Poisson's ratio is $5e^5$ MPa, 0.3. For bolt, elastic modulus and Poisson's ratio is $2e^5$ MPa, 0.3.

The concrete damaged plasticity model is used to simulate the behavior of concrete [15], which considers the restraints of the outer steel pipe. Meanwhile, the strain rate under dynamic loading must be considered. The model in CEB-FIP, 1993 [12] is employed:

$$\sigma_d / \sigma_s = (\dot{\epsilon}_d / \dot{\epsilon}_s)^{1.026\alpha} \quad \dot{\epsilon}_d \leq 30s^{-1} \quad (2)$$

$$f_{td} / f_{ts} = \begin{cases} (\dot{\epsilon}_d / \dot{\epsilon}_s)^\delta & \dot{\epsilon}_d \leq 1s^{-1} \\ \beta(\dot{\epsilon}_d / \dot{\epsilon}_s)^{1/3} & \dot{\epsilon}_d > 1s^{-1} \end{cases} \quad (3)$$

where, σ_d is concrete's compressive strength under impact loading, σ_s is concrete's static compressive strength, $\dot{\epsilon}_d$ is the dynamic strain rate, $\dot{\epsilon}_s$ is the strain rate under static loading. Under pressure, $\dot{\epsilon}_s = -30 \times 10^{-6} s^{-1}$, while in tension, $\dot{\epsilon}_s = 1 \times 10^{-6} s^{-1}$. f_{td} is tensile strength of concrete under impact loading, f_{ts} is tensile strength of concrete under static loading. And $\alpha = 1/(5+9f_c'/f_{co})$, $f_c' = f_{ck} + 8(N/mm^2)$, $f_{co} = 10(N/mm^2)$, where f_{ck} is the characteristic value of concrete compressive strength. $\log \beta = 6\delta - 2$, $\delta = 1/(1+8f_c'/f_{co})$; In this paper, for concrete, adopt C40, $E_c = 4370f_c'^{1/2}$ MPa, Poisson's ratio is 0.2. Also, since the inertial force, the density of steel is taken as 7850 kg/m^3 , and the density of concrete is 2500 kg/m^3 .

2.2 Interface contact

The contacts of steel – hammer, steel – concrete, steel – supporters and supporters – bolts are made of general contact, which in normal take hard contact, in tangential take the Columbia Friction model to simulate the relative slip. The friction factors of Coulomb friction were recommended by Han [15].

2.3 Boundary and initial conditions

Figure 1 show the fixed-simply boundary condition. The shapes of simply supporter and fixed supporter are shown in figure 1. In the fixed supporter, the upper part is connected with the lower part by eight bolts with 20mm diameters. The bottoms of imply supporter and fixed supporter are fully constrained

In this model, hammer is 1mm up to the upside of the specimen, its mass is 203.9kg and the initial velocity of hammer is given according to different impact energy.

2.4 Element type and mesh

In the FEA model, steel tubes are simulated by using 4-node shell elements with reduced integration, hammer uses the 4-node discrete rigid shell elements with reduced integration, while the other parts are modeled by the 8-node solid elements.

After comparing the mesh quality and calculation time of different mesh sizes, this model adopt local refinement, in the non- encrypted area the mesh size is 20mm and in the encrypted area the mesh size is 5mm. Figure 2 shows the mesh of this FEA model.

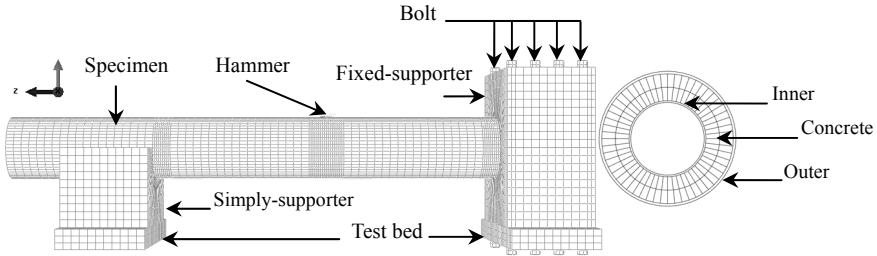


Figure 1: Abaqus model and mesh.

3 Results of finite element analysis (FEA)

Four circular CFDST members are simulated, the length of all specimens is 1500mm, the diameters of outer steel tube and inner steel tube are 170mm and 100mm respectively, and the thickness of outer steel tube and inner steel tube are 3mm and 2mm respectively. The detailed information of each specimen is presented in Table 1, where “F” for fixed supporters and “S” for simply supporters, while the number denotes the height of the hammer. Take “s-FS3” for example, denotes that the hammer drop at a height of 3m under fixed and simply supported. Then, “ H ”, “ V_0 ” and “ E_0 ” represent the height, the velocity, and the energy of the impact, “ F_{stab} ”, “ t ” represent plateau value and time of the impact force, and “ Δ ” is the ultimate lateral deflection of specimen at mid-span.

Table 1: Specimen information.

No.	H (m)	V_0 (m/s)	E_0 (kJ)	F_{stab} (kN)	t (ms)	Δ (mm)
FS3	3	7.67	5.99	293.71	8.42	7.26
FS5	5	9.9	9.99	308.34	10.56	13.81
FS7	7	11.71	13.99	318.4	10.72	21.51
FS9	9	13.28	17.99	322.44	10.97	29.77

3.1 The failure modes

In Figure 2 the predicted typical failure model of CFDST is shown. It can be observed that the failure model include the integer bending deformation and local buckling of steel tube on the upside of CFDST at the mid-span.

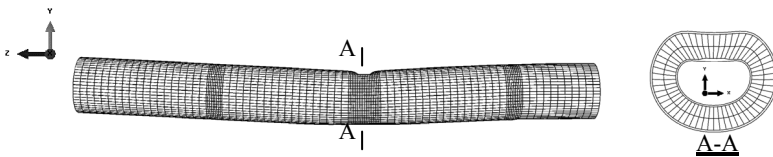


Figure 2: Failure modes of CFDST member.

3.2 Impact force and deflection

Figure 3 compares the impact force between different impact energy of dynamic loads and static loads. It can be seen that with the same static flexural capacity (M_u), the resistant capacity of the specimen under impact is 4%–14% higher than that under static impact. M_u reference to the practical formula proposed by Hang Hong^[16], and it is related to the section and material only.

$$M_u = \gamma_{m1} W_{scm} f_{scy} + \gamma_{m2} W_{sif} f_{yi} \quad (4)$$

As can be seen from the curves of figure 3, plateau value (F_{stab}) and time (t) of the impact force increases along with the rise of the velocity (V_0). And at the impact height of 9m there is a distinct peak impact force. It certifies the damage of CFDST under impact is ductile failure, these specimens have well anti-impact performance.

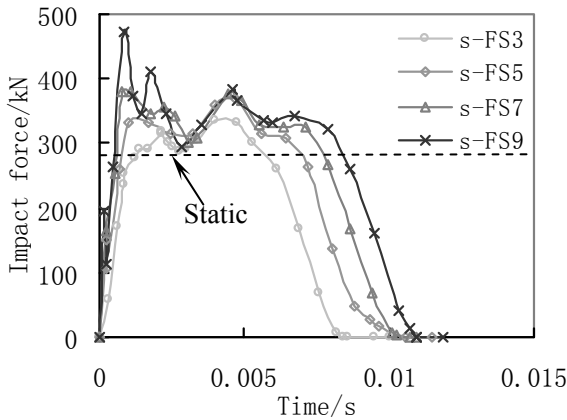


Figure 3: Contrast of F_{stab} under static and impact load.

Figure 4 compares the lateral deflection of specimen at mid-span under different impact velocity in FEA model. This figure shows that the deflection (Δ) increases with the rise of the velocity (V_0). Reference to the curves, the members appeared total deformation in 8ms, the specimens rebounded after the max deflection until final equilibrium.

3.3 Dynamic response analysis of the whole process

Take the simulate result of specimen s-FS9 as the example to analyze the work mechanic and full range of the dynamic response.

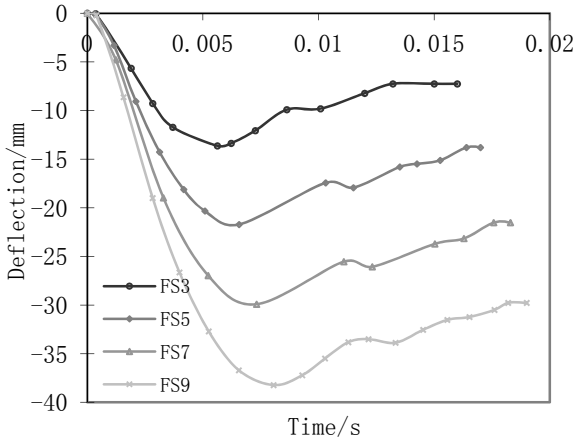


Figure 4: Contrast of deflection under different height.

Figure 5 shows the dimensionless results of impact force (F), deflection (Δ), the velocity of hammer (V_0) and the velocity of member (V). Obviously, these time-curves can be divided into the following four stages:

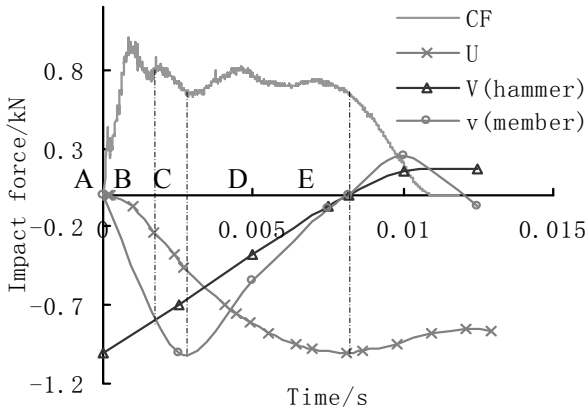


Figure 5: Impact force (F), deflection (Δ), velocity (V) versus time.

First, peak stage (from point A to B): During this stage, the impact force increases rapidly, the velocity of the hammer decreases while the velocity of the CFDST member increases. At the end of this period, the hammer and the member achieve the same speed, the impact force rises to peak, meanwhile the member’s initial deformation appears.

Second, descent stage (from point B to C): At this stage, the speed of hammer continues to reduce while the speed of member continues to increase until to the maximum speed. Due to elastic recovery of the local deformation, the hammer and specimen don't separate, but the impact force declines for a short time.

Third, Recovery – Platform stage (from point C to D): In this phase, the speed of hammer decreases rapidly and rebound relatively, which cause the impact force come to peak again. The speed of hammer and CFDST member get convergence at the platform of the impact force.

Last, unloading stage (from point D to E): At the point D, the speed of hammer and CFDST member reduce to zero, the displacement of the specimen rise to the limits. During this stage, the CFDST member rebounds while the impact force gradually unloaded to zero.

4 Conclusions

- 1) With the same static flexural capacity (M_u), the resistant capacity of the specimen under impact is 4%-14% higher. Plateau value (F_{stab}) and time (t) of the impact force increases with the rise of the velocity (V_0). The deflection (Δ) increases with the rise of the velocity (V_0).
- 2) The failure model include the integer bending deformation and local buckling of the steel tube on the upside of CFDST at the mid-span
- 3) The full range of the dynamic response based on FEA model proves that time-curves can be divided into four stages: Peak stage, Descent stage, Recovery – Platform stage, Unloading stage.

References

- [1] Tao Z, Yu Q. New composite columns: Test, Theory and Methods. Sciencep. BJ. 2006.
- [2] Wang R. Dynamic response and damage failure of CFST under lateral impact. PhD thesis of Taiyuan University of Technology. 2008.
- [3] Lu XZ, He ST, Huang SN. Failure Mechanism, Design methods and protective measures of superstructure under impact. China Architecture & Building Press. BJ. 2011.
- [4] Maria Garlock, Ignacio Paya-Zaforteza, Venkatesh Kodur, Li G. Fire hazard in bridges: Review, assessment and repair strategies. Engineering structures, 35(07), pp. 89-98, 2012.
- [5] Chen ZY, Luo JQ, Pan XW. Performance of CFST as protective structures. Earthquake and Antiknock Engineering Research Center of Tsinghua University. BJ. 1986.
- [6] Xiao Y, Shan JH, Zheng Q, Chen BS, Shen YL. *Experimental studies on concrete filled steel tubes under high strain rate loading*. Journal of Materials in Civil Engineering, 21(10), pp. 569-577, 2009.
- [7] Huo JS, Ren XH, Xiao Y. *Impact behavior of concrete-filled steel tubular stub columns under ISO-834 standard fire*. China Civil Engineering Journal. 45(04), pp. 9-20, 2012.



- [8] Bambach M R. *Design of hollow and concrete filled steel and stainless steel tubular columns for transverse impact loads*. Thin-Walled Structures, 49(10), pp. 1251-1260, 2011.
- [9] Wang Rui, Han LH, Hou CC. *Behaviour of concrete filled steel tubular (CFST) members under lateral impact: experiment and FEA model*. Journal of construction steel research, 80 (01), pp. 188-201, 2013.
- [10] Hou CC. *Study on Performance of Circular Concrete-filled Steel Tubular (CFST) Members under Low Velocity Transverse Impact*. Journal of Tsinghua University. 2012.
- [11] Tao Z, Han LH. *Development in the research of concrete filled double-skin steel tubes [J]*. Journal of Harbin Institute of Technology. 35, pp. 144-146, 2003.
- [12] Huang H, Tao Z, Han LH. *Mechanism of concrete-filled double-skin steel tubular columns (CHS inner and CHS outer) subjected to axial compression [J]*. Industrial Construction Vol. 36, No. 11, 2006. 11-14.
- [13] Chen XJ, Chen MC, Huang C. *Hysteretic model of concrete-filled double-skin steel tubular bending members*. Railway Engineering. pp. 141-144, 2011(4).
- [14] Huang H, Chen MC, Huang BJ. *Twist study of concrete-filled double-skin steel tubular*. Journal of experimental mechanics 27(3), pp. 288-294, 2012.
- [15] Han LH. *Concrete-filled steel tubular structures – theory and application*. Sciencep. BJ. 2007.
- [16] Huang H. *Behavior of concrete filled double-skin steel tubular beam-columns*. PhD thesis of Fuzhou University. 2008.
- [17] Hibbitt, Karlsson & Sorensen Inc *ABAQUS/Explicit User's Manual*. Vision 6.10. Hibbitt, Karlsson & Sorensen Inc; 2005.

